^{99m}Tc-HMPAO–Labeled Autologous Versus Heterologous Leukocytes for Imaging Infection

Stefan Gratz, MD[1,2]; Huub J.J.M. Rennen, MSc[1]; Otto C. Boerman, PhD[1]; Wim J.G. Oyen, MD[1]; Peter Mast[3]; Thomas M. Behr, MD[2]; and Frans H.M. Corstens, MD[1]

[1]Department of Nuclear Medicine, University Medical Center Nijmegen, Nijmegen, The Netherlands; [2]Department of Nuclear Medicine, Philipps University Marburg, Marburg, Germany; and [3]Department of Hematology, University Medical Center Nijmegen, Nijmegen, The Netherlands

Radiolabeled autologous leukocytes are the gold standard for imaging infectious foci in patients. Good results have also been reported for radiolabeled heterologous leukocytes from noninfected donors. Until now, the 2 methods have not been directly compared. In this study, we compared the infection-imaging potential of ^{99m}Tc-hexamethylpropyleneamine oxime (HMPAO)–labeled autologous granulocytes with that of ^{99m}Tc-HMPAO–labeled granulocytes from either infected or noninfected donors in rabbits with *Escherichia coli* infection. **Methods:** The radiolabeled granulocyte preparations were studied in rabbits with an *E. coli* infection in the left calf muscle. The soft-tissue infections were scintigraphically visualized after injection of 18 MBq of either ^{99m}Tc-HMPAO purified autologous granulocytes or radiolabeled purified heterologous granulocytes from infected or noninfected donor rabbits. Gamma camera images were acquired at 2 min and at 1, 2, and 4 h after injection. After the last image, the rabbits were killed and uptake of the radiolabel in the dissected tissues was determined. **Results:** The ^{99m}Tc-HMPAO autologous granulocytes and heterologous granulocytes from infected donors accurately revealed the infectious focus in the calf muscle at 2 h after injection. At 4 h after injection, a significantly better ($P < 0.05$) delineation of the infection was established with the ^{99m}Tc-HMPAO autologous granulocytes and ^{99m}Tc-HMPAO heterologous granulocytes from the infected rabbits than with the heterologous granulocytes from noninfected donors. With both cell preparations, the intensity of uptake in the infected calf muscle continuously increased until 4 h after injection. The ^{99m}Tc-HMPAO heterologous granulocytes from noninfected donors showed no significant increase in contrast after 2 h after injection. Absolute uptake in the infected calf muscle was much higher for ^{99m}Tc-HMPAO autologous granulocytes (7.81 ± 1.21 percentage injected dose [%ID]) and ^{99m}Tc-HMPAO heterologous infected granulocytes (8.91 ± 1.92 %ID) than for the radiolabeled heterologous noninfected granulocytes (2.32 ± 0.75 %ID) ($P < 0.04$) at 4 h after injection. The ratio of infected muscle to noninfected contralateral muscle was significantly higher for ^{99m}Tc-HMPAO autologous granulocytes and ^{99m}Tc-HMPAO heterologous granulocytes from infected donors than for ^{99m}Tc-HMPAO heterologous granulocytes from noninfected donors (5.53 ± 1.09, 3.86 ± 0.75, and 1.86 ± 0.31, respectively; $P < 0.05$). **Conclusion:** For nuclear medicine imaging of infection, purified granulocytes derived from infected rabbits are superior to purified granulocytes derived from noninfected donor rabbits. In addition, autologous granulocytes gave similar results to heterologous granulocytes from infected donor rabbits, suggesting the need for intrinsic cell activation for specific granulocyte migration.

Key Words: radiolabeled leukocytes; ^{99m}Tc-HMPAO; autologous granulocytes; heterologous granulocytes

Thakur et al. (*1–3*) were the first to describe the successful use of ^{111}In-labeled autologous purified granulocytes for the localization of abscesses in febrile patients. Since then, this method has become the gold standard for imaging of infection in nuclear medicine. Radiolabeled autologous granulocytes allow rapid visualization of infected and inflamed foci within 1–4 h after intravenous reinjection. In other studies, ^{111}In-labeled purified granulocytes were compared with ^{111}In-labeled mixed leukocytes. The results showed that the detection of acute infection with these preparations was equivalent (*4*). Various clinical trials showed that ^{111}In-labeled (pure or mixed) leukocytes allowed accurate evaluation of patients suspected of having inflammatory disease. In these studies, the sensitivity of ^{111}In-leukocytes for detecting infectious foci was 84%–96%, and the specificity exceeded 96% (*5*).

In patients with neutropenia, the situation is more complicated. The small number of circulating leukocytes does not allow isolation of enough labeled cells for reinjection. In these patients, the use of radiolabeled granulocytes derived from noninfected donors (*6–9*) for imaging infection has been shown to be feasible. The method relied simply on ABO/Rh blood group matching between donor and recipient. The investigators indicated that this approach had the advantages of not affecting the functionality of the donor leukocytes, as would chemotherapy (*9*); of eliminating the need to perform a large venesection on the patient to harvest sufficient neutrophils (*9*); and of lacking a definite risk of contamination to personnel who perform the labeling or

even inadvertent cross-contamination between patients (*10–12*). In the patients who received the donor cells, no adverse reactions were observed.

[111]In-labeled donor-leukocyte scans have successfully been used in various clinical trials (*6–9*). So far, it is unknown how ^{111}In-labeled donor leukocytes and radiolabeled autologous leukocytes compare for imaging infection. The aim of this study was to compare the imaging performance of ^{99m}Tc-hexamethylpropyleneamine oxime (HMPAO)–labeled autologous granulocytes with that of ^{99m}Tc-HMPAO–labeled heterologous granulocytes derived from infected and noninfected donor rabbits.

MATERIALS AND METHODS

Animal Model

Abscesses were induced in the left thigh muscle of 16 female New Zealand rabbits (body weight range, 2.4–2.7 kg) with 0.5 mL of a suspension of *Escherichia coli* (2×10^{11} colony forming units per milliliter). During the procedure, the rabbits were anesthetized with a 0.6-mL subcutaneous injection of a mixture of 0.315 mg/mL fentanyl and 10 mg/mL fluanisone (Hypnorm; Janssen-Cilag Ltd., Buckinghamshire, U.K.). After 24 h, when swelling of the muscle was apparent, 3 groups of 5 animals (groups A, B, and C) were formed. The experiments were performed in accordance with the guidelines of the local animal welfare committee.

Granulocyte Isolation

Granulocytes were isolated according to the method of Lillevang et al. (*13*), with minor modifications (*14*). Briefly, the blood was mixed with a one-tenth volume of 6% dextran (267 kDa) + acid-citrate-dextrose solution in 0.9% NaCl and allowed to settle for 1 h at room temperature. The leukocyte-rich supernatant was layered carefully on a one-third volume of density medium (Nycoprep; Nycomed, Oslo, Norway [14.1% Nycodenz (Nycomed), 0.3% NaCl, 5 mmol/L tricine/NaOH, pH 7.2, density = 1.077 g/mL, osmolality = 265 mosm]) and centrifuged for 15 min at 600*g*. The plasma above the mononuclear cells, the mononuclear band, and the density medium above the granulocyte pellet were carefully removed. The pellet was washed with 5 mL Hanks' balanced salt solution with 10% autologous plasma and centrifuged for 10 min at 50*g*. The cell pellet was resuspended in 1.5 mL Hanks' balanced salt solution, 10% rabbit plasma. After this purification procedure, the granulocyte purity exceeded 95% for each preparation.

Cell Labeling

Between 81 and 83 MBq freshly prepared ^{99m}Tc-HMPAO were added to each of the autologous (*n* = 5) and heterologous infected (*n* = 5) or noninfected (*n* = 5) cell suspensions. The cells were incubated at room temperature for 30 min and centrifuged for 10 min at 50*g*. The pellet was resuspended in 5 mL cell-free autologous plasma. Labeling efficiency (cell-associated activity/total activity added) was 40%–50% for the different granulocyte preparations. The functional integrity of labeled granulocytes was evaluated by their in vivo performance, including transit through the lungs and uptake into the liver and spleen. A dose of 18 MBq ^{99m}Tc-labeled granulocytes was administered intravenously to each rabbit.

The right-ear artery of each rabbit was cannulated, and 20 mL blood were drawn from each rabbit into an acid-citrate-dextrose tube (containing 2.5 mL 6% dextran [267 kmol; Sigma-Aldrich, Zwijndrecht, The Netherlands] + 4 mL acid-citrate-dextrose solution [NPBI-Biotrans GmbH, Dreieich, Germany] per 20 mL blood). The leukocyte count in the full blood of the rabbits ranged from 7.7 to 8.2 × 10^{9}/L, with approximately 70% granulocytes. After granulocyte isolation, the cell count ranged from 8.2 to 10.0 × 10^{9}/L (measured in the same volume), with >95% granulocytes.

FACS Analysis

For cell counting by fluorescence-activated cell sorter (FACS) analysis, an H3* RTX hematology analyzer (Bayer Diagnostics, Tarrytown, NY) was used. This FACS analyzer screens 2 parameters: the peroxidase channel, for measurement of the peroxidase activity in the cells as a measure of cell diameter, and the basophilic method, for measurement of cell granularity.

To differentiate the rabbit blood cells, a FACS analyzer that had been tuned for the evaluation of human blood was tuned for the evaluation of rabbit blood using a different set of gain factors. The final estimate of blood count was made through comparison of the FACS results with the results of manual counting. Consequently, the total number of white blood cells was evaluated using the basophilic method, whereas the differential blood count was roughly estimated using peroxidase channel measurements. Microscopic evaluation of blood smears was used for final confirmation.

Gamma Camera Imaging and Data Analysis

For imaging, rabbits were immobilized in a mold and placed prone on the gamma camera. Five rabbits of group A were injected with 18 MBq ^{99m}Tc-HMPAO autologous purified granulocytes through the ear vein. Ten rabbits were injected with 18 MBq ^{99m}Tc-HMPAO heterologous purified granulocytes, which were derived from infected donor rabbits (group B, *n* = 5) or from noninfected donor rabbits (group C, *n* = 5). Three rabbits of each group were used for gamma camera imaging. At 2 min and at 1, 2, and 4 h after injection, images were recorded with a single-head gamma camera (Orbiter; Siemens Medical Systems, Inc., Hoffman Estates, IL) equipped with a parallel-hole low-energy all-purpose collimator. Images were obtained with a 15% symmetric window over the 140-keV energy peak of [99m]Tc. After acquisition of 300,000 counts, the images were digitally stored in a 256 × 256 matrix.

For quantitative analysis of the scintigraphic images, regions of interest were drawn over the abscess and the noninfected contralateral thigh muscle (background). Abscess-to-background ratios, lung-to-liver ratios, and uptake measurements for kidney, liver, and spleen were calculated.

After the final images had been acquired, the rabbits were killed with an overdose of sodium phenobarbital and the biodistribution of the radiolabeled tracers was determined. Blood was obtained by cardiac puncture. Tissues (lung, liver, spleen, kidney, small intestine, colon, infected left calf muscle, and noninfected contralateral muscle) were dissected and weighed, and the radioactivity was measured in a shielded well scintillation γ-counter (Wizard; Pharmacia-LKB, Uppsala, Sweden). To correct for decay and to permit calculation of uptake of the radiolabeled leukocyte preparation in each organ as a fraction of the injected dose, aliquots of the injected dose (1%) were counted simultaneously. The uptake results were expressed as percentage injected dose per gram (%ID/g) or, for the abscess, percentage injected dose (%ID).

Statistical Analysis

All uptake values are given as mean $\pm$ 1 SEM. One-way ANOVA was used to compare uptake in the infected calf muscle with uptake in the noninfected contralateral muscle, using the InStat software package (version 3.00; GraphPad Software, San Diego, CA). The level of significance was set at $P < 0.05$.

RESULTS

A soft-tissue infection developed in the left thigh muscle of all rabbits ($n = 16$; 15 for imaging, 1 for granulocyte preparation) within 24 h after bacterial inoculation. Swelling of the left thigh muscle and redness of the skin were grossly apparent in all rabbits. Cross-sections of the abscess sample macroscopically showed encapsulated purulent material. Scintigraphic images of the radiolabeled granulocyte preparations at 2 min and at 1, 2, and 4 h after injection are shown in Figure 1.
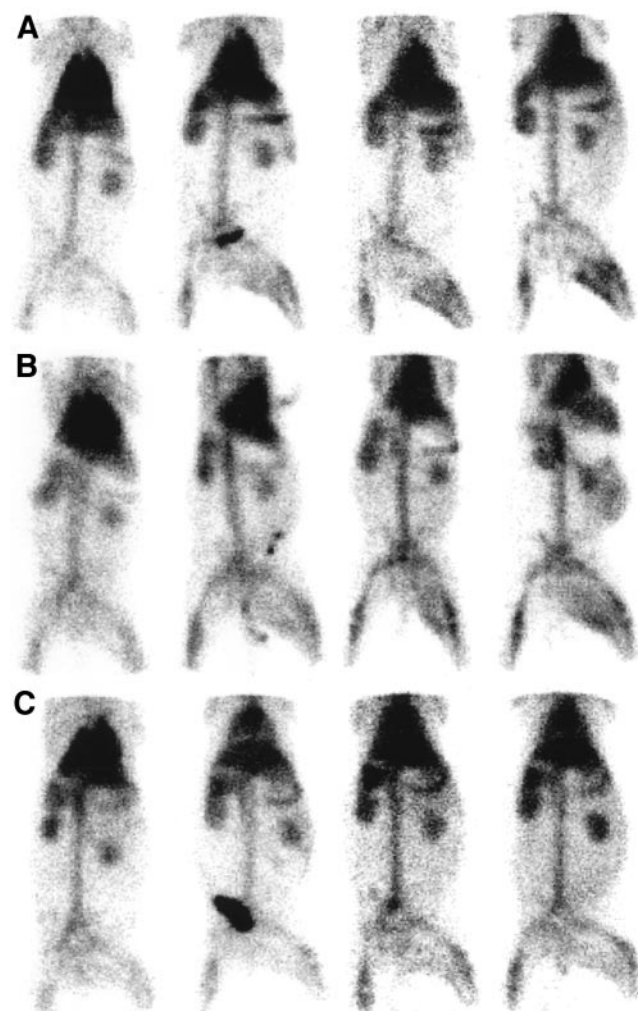

FIGURE 1. Scintigrams of rabbits with *Escherichia coli* infection in left calf muscle imaged at (from left to right) 2 min and at 1, 2, and 4 h after injection of [99mTc]-HMPAO autologous purified granulocytes (A) and [99mTc]-HMPAO-purified granulocytes derived from infected (B) and noninfected (C) donor rabbits.

Quantitative analysis of the scintigrams of [99mTc]-HMPAO autologous granulocytes and of [99mTc]-HMPAO heterologous granulocytes from infected and noninfected donors showed a rapid initial lung transit and low liver and spleen uptake, indicating that the [99mTc]-labeling procedure did not harm granulocyte function (Fig. 2).

[99mTc]-HMPAO autologous granulocytes and [99mTc]-HMPAO heterologous granulocytes from infected donors nicely showed the infection as early as 2 h after injection. Contrast between abscess and background improved on the subsequent scintigrams with both preparations. Uptake in the abscess was equal for [99mTc]-HMPAO autologous granulocytes (0.19 ± 0.08 %ID/g at 4 h after injection) and [99mTc]-HMPAO heterologous granulocytes from infected donors (0.19 ± 0.04 %ID/g at 4 h after injection) and led to good scintigraphic delineation of the infected thigh muscle. In contrast, [99mTc]-HMPAO heterologous granulocytes from noninfected donors showed low uptake in the infected muscle at 1–2 h after injection, and no further increase in uptake was observed on the later scintigrams.

The kinetics of abscess uptake derived from region-of-interest analysis of the 3 granulocyte preparations at various times are summarized in Figure 3. [99mTc]-HMPAO autologous granulocytes and [99mTc]-HMPAO heterologous granulocytes from infected donors continuously increased with time and reached a maximum at 4 h after injection (7.81 ± 1.21 %ID and 8.91 ± 1.92 %ID, respectively), whereas [99mTc]-HMPAO heterologous granulocytes from noninfected donors reached a maximum between 2 and 4 h after injection (2.32 ± 0.75 %ID) and then decreased. The abscess-to-background ratios for [99mTc]-HMPAO autologous granulocytes and [99mTc]-HMPAO heterologous granulocytes from infected donors were highest at 4 h after injection, at 5.53 ± 1.09 and 3.86 ± 0.75, respectively. For [99mTc]-HMPAO heterologous granulocytes from noninfected donors, the tumor-to-background ratio did not change with time, at 1.16 ± 0.14, 1.50 ± 0.27, and 1.86 ± 0.31 at 1, 2, and 4 h, respectively, after injection (Fig. 4).

The biodistribution data for the 3 radiolabeled granulocyte preparations at 4 h after injection are given in Table 1. In accordance with the scintigraphic results, [99mTc]-HMPAO autologous granulocytes and [99mTc]-HMPAO heterologous granulocytes from infected donors showed significantly higher uptake in the infectious focus at 4 h after injection than did [99mTc]-HMPAO heterologous granulocytes from noninfected donors (0.19 ± 0.08, 0.19 ± 0.04, and 0.06 ± 0.04 %ID/g, respectively; $P < 0.05$). Uptake of all 3 radiolabels was comparatively low in normal muscle tissue. Consequently, the abscess-to-muscle ratio for [99mTc]-HMPAO autologous granulocytes (108 ± 62) was as high as that for [99mTc]-HMPAO heterologous granulocytes from infected donors (108 ± 53) and significantly higher than that for [99mTc]-HMPAO heterologous granulocytes from noninfected donors (39 ± 22) ($P < 0.05$). Each of the 3 preparations showed comparably high uptake in the spleen (between 1.36 ± 0.47 and 1.59 ± 0.26 %ID/g). Liver
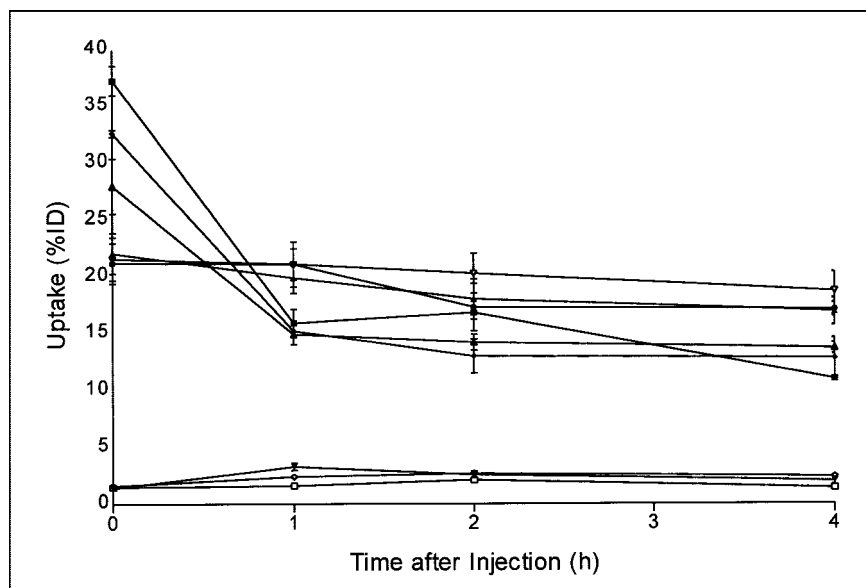
FIGURE 2. Quantitative analysis (mean ± SD) of scintigrams of rabbits shows clearance from lungs (top set of 3 lines), liver (middle set of 3 lines), and spleen (bottom set of 3 lines). Top line of each set is data for injection of ^{99m}Tc-HMPAO autologous granulocytes, middle line of each set is data for injection of ^{99m}Tc-HMPAO heterologous granulocytes from infected donors, and bottom line of each set is data for injection of ^{99m}Tc-HMPAO heterologous granulocytes from noninfected donors. Whole-body activity measured at 2 min after injection was set at 100%; error bars represent SD.

uptake was similar for all 3 preparations (Table 1). The 3 preparations showed comparably low blood levels, resulting in low uptake in background tissues (muscle and small intestine). Localization in most other tissue samples was remarkably similar. Based on regions of interest, an over-time increase in renal ^{99m}Tc activity with all 3 labeled granulocyte preparations was noted (from 1.5 to 3.0 %ID for autologous granulocytes, from 2.0 to 3.1 %ID for heterologous infected granulocytes, and from 2.7 to 4.1 %ID for heterologous noninfected granulocytes; $P < 0.17$), reflecting excretion of ^{99m}Tc-HMPAO complexes eluted from labeled cells. Kidney uptake was similar for the 3 preparations.

DISCUSSION

The paucity of diagnostic clues in febrile patients and the limitations of current radiopharmaceuticals stimulate a search for agents that can rapidly and effectively reveal infectious foci. Especially in granulocytopenic patients, the lack of such an agent may cause clinical problems. ^{111}In-labeled leukocytes represent the gold standard for specifically locating abscess formations ([1,4,15,16]). In most patients, autologous purified granulocytes or autologous mixed leukocyte populations have been used as cellular compounds for radiolabeling. In obtaining images using radiolabeled white blood cells, the feasibility of isolating purified granulocytes or mixed leukocyte populations depends on the patient's leukocyte count or immune status. Alternative methods to detect infection include the use of ^{67}Ga-citrate ([17–20]), ^{99m}Tc-labeled granulocyte-specific antibodies ([21]), and radiolabeled donor leukocytes ([6–9]). ^{67}Ga-citrate has proven to be highly sensitive in detecting infectious tissue alterations, with a positive predictive value of 93% ([20]), but has shown low specificity, mainly because
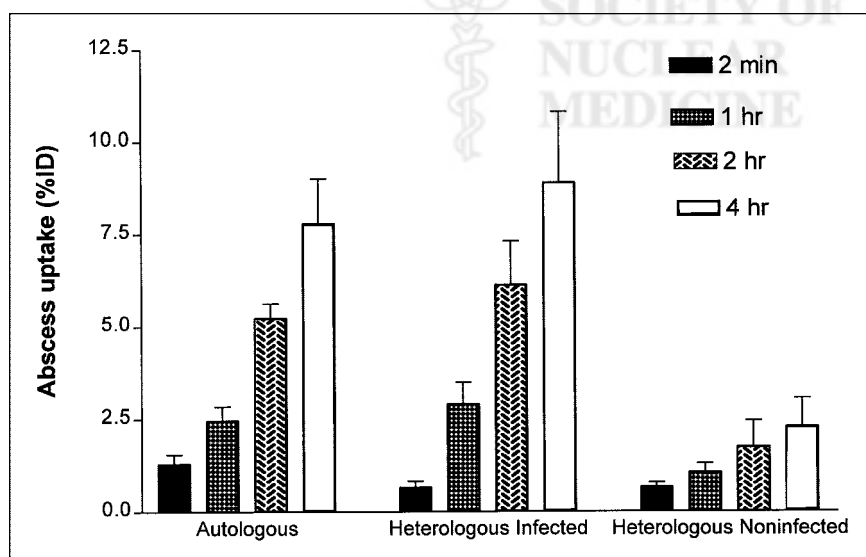

FIGURE 3. Abscess uptake (%ID) of ^{99m}Tc-HMPAO autologous granulocytes and of ^{99m}Tc-HMPAO heterologous granulocytes from infected and noninfected donors at 2 min and at 1, 2, and 4 h after injection
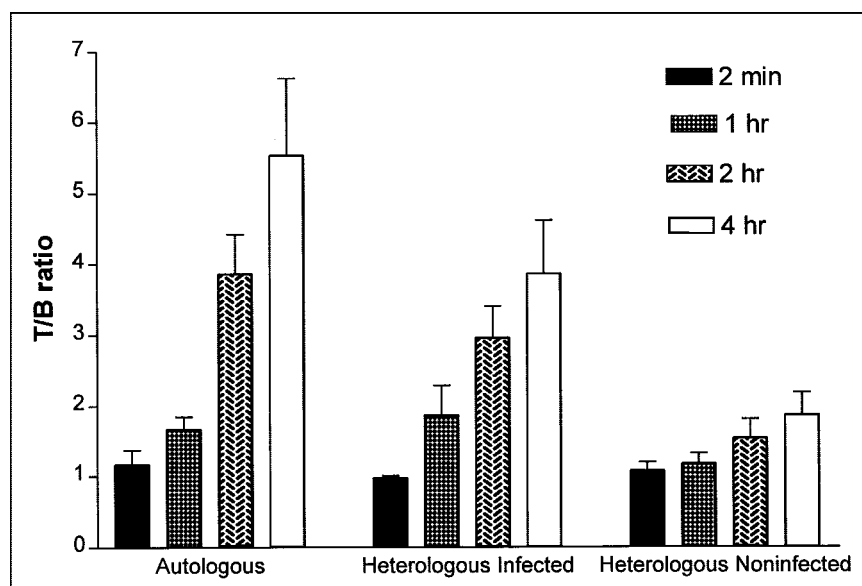
FIGURE 4. Abscess-to-background (non-infected contralateral muscle) ratio (T/B ratio) at 2 min and at 1, 2, and 4 h after injection of ^{99m}Tc-HMPAO autologous granulocytes and of ^{99m}Tc-HMPAO heterologous granulocytes from infected and noninfected donors.

this agent does not allow differentiation between infection and malignancy. Prvulovich et al. (21) prospectively studied the value of immunoscintigraphy with ^{99m}Tc-labeled anti-granulocyte monoclonal antibody (BW250/183) in HIV (type 1) antibody–positive patients presenting with fever but no localizing symptoms or signs. ^{99m}Tc-antigranulocyte antibody imaging correctly identified the sites of infection in only 5 (22%) of 23 patients. Sixteen foci of infection were not localized by ^{99m}Tc-antigranulocyte immunoscintigraphy (false-negative findings). Problems also have been noticed in immunodeficient patients when imaged with donor radiolabeled leukocytes (6–9), and the overall results were mediocre compared with those for healthy volunteers imaged with autologous radiolabeled leukocytes (22). Anstall et al. (6) described 8 patients who were receiving chemotherapy and had superinfection, and O'Doherty et al. (9) described 4 patients who had AIDS and superinfection. Both authors

reported a low fraction of positive findings for scans obtained with ^{111}In-labeled donor leukocytes. The authors believed that the limited sensitivity reflected hospital practice in performing CT and sonography before leukocyte scanning or that no localized inflammatory focus became clinically evident over that time. Better results were reported by Dutcher et al. (7), who saw positive findings as early as 30 min after injection. But in the 14 patients examined, all sites of infection were known beforehand. In summary, the studies suggested that radiolabeled leukocyte imaging appears suboptimal in immune-compromised patients.

Our study showed that ^{99m}Tc-HMPAO–labeled granulocytes derived from autologous or heterologous infected animals have better characteristics for localizing a bacterial infection than do ^{99m}Tc-HMPAO heterologous granulocytes from noninfected donors. The highest abscess uptake and

TABLE 1
Biodistribution in Rabbits with *E. coli* Abscess 4 Hours After Injection

	^{99m}HMPAO granulocytes		
Site	Autologous	Heterologous infected	Heterologous noninfected
Blood	0.13 ± 0.05	0.12 ± 0.02	0.11 ± 0.03
Muscle	0.002 ± 0.010	0.002 ± 0.010	0.001 ± 0.010
Abscess	0.19 ± 0.08	0.19 ± 0.04	0.06 ± 0.04
Abscess*	1.96 ± 0.49	2.29 ± 0.43	1.21 ± 0.47
Lung	0.59 ± 0.25	0.51 ± 0.21	0.26 ± 0.09
Speen	1.36 ± 0.47	1.30 ± 0.32	1.59 ± 0.26
Kidney	0.13 ± 0.03	0.13 ± 0.03	0.12 ± 0.02
Liver	0.15 ± 0.01	0.18 ± 0.04	0.17 ± 0.02
Intestine	0.02 ± 0.01	0.01 ± 0.01	0.01 ± 0.01
Infected muscle	108 ± 62	108 ± 53	39 ± 22
Infected blood	1.96 ± 1.12	1.63 ± 0.30	0.74 ± 0.83

*Data for this site are %ID (mean ± SD); data for other sites are %ID/g (mean ± SD).

abscess-to-muscle ratios were obtained with ^{99m}Tc-HMPAO autologous granulocytes and ^{99m}Tc-HMPAO heterologous granulocytes from infected donors, exceeding the value for ^{99m}Tc-HMPAO heterologous granulocytes from noninfected donors by 67% and 52%, respectively. Because all 3 preparations showed comparably low blood levels, with low uptake in background tissues (muscle and small intestine) and undisturbed granulocyte function, the better performance and higher uptake of ^{99m}Tc-HMPAO autologous granulocytes and ^{99m}Tc-HMPAO heterologous granulocytes from infected donors in the infected muscle appears to be caused by the better chemotactic properties of granulocytes from infected animals. The good performance of the ^{99m}Tc-HMPAO heterologous granulocytes from infected donors, compared with the ^{99m}Tc-HMPAO heterologous granulocytes from noninfected donors, was remarkable. These observations suggest that the in vivo environment of leukocytes before isolation determines their migratory capacity. An explanation may be the chemotactic activation of infected granulocytes, because in patients with inflammatory bowel disease, chemotactic factors generated in the interstitial tissue attract neutrophils from the circulation into the inflammatory site and thus infiltration of neutrophils in the interstitial tissue, contributing to accumulation and activation of neutrophils in the infected mucosa (23). It has been postulated that emigration of leukocytes to perivascular infected tissue is caused not only by the chemotactic proinflammatory cytokine response alone (24) but also by the state of activation of lymphocytes and the expression of adhesion molecules on vascular endothelium or intensive expression on granulocytes (25). Another explanation for the different in vivo behavior of granulocytes may be the physiologic distribution of granulocytes in the blood. Approximately half of granulocytes in the peripheral blood are freely circulating, whereas the other half form the marginating pool in the circulation (26–30). Marginating granulocytes are particularly mobilized by subtle stimuli such as exercise (5). For this reason, donor granulocytes harvested from a normal, nonmarginating pool have relatively poor migrating capacity. Furthermore, studies of emigration response have also shown that 30–40 min are required after stimulation before normal neutrophils leave the venules (5).

Future investigations will have to focus on improving the migration capacity of heterologous noninfected granulocytes by, for instance, in vitro incubation with biologically active factors (such as proinflammatory cytokines or granulocyte growth-stimulating factors) for further improving white cell imaging of infection in humans.

This study showed that donor leukocytes can successfully be used to trace areas of inflammation. Our data suggest that chemotactic activation of granulocytes is of crucial importance and determines the ability of granulocytes to localize infection and inflammatory foci earlier than can normal, nonactivated cells. Our studies have shown that images of ^{99m}Tc-HMPAO heterologous granulocytes from noninfected donors did not improve between 4 and 24 h after injection

(31–33). The results of this study contribute to a better understanding of biokinetic granulocyte migration and warrant further studies on the use of donor leukocytes for imaging infection.

CONCLUSION

In a rabbit model with *E. coli* soft-tissue infection, ^{99m}Tc-HMPAO autologous granulocytes and ^{99m}Tc-HMPAO heterologous granulocytes from infected donors provided good visualization of abscess formation early after intravenous injection and showed higher focal uptake and target-to-nontarget ratios than did ^{99m}Tc-HMPAO heterologous granulocytes from noninfected donors. These results indicate that autologous and heterologous activated granulocytes are more useful in the evaluation of scintigraphic imaging of infection than are nonactivated donor granulocytes. Further studies on the use of donor granulocytes are therefore warranted.

REFERENCES

1. Thakur ML, Segal AW, Louis L, Welch MJ, Hopkins J, Peters TJ. Indium-111-labeled cellular blood components: mechanism of labeling and intracellular location in human neutrophils. *J Nucl Med.* 1977;18:1022–1026.
2. Thakur ML, Lavender JP, Arnot RN, Silvester DJ, Segal AW. Indium-111-labeled autologous leukocytes in man. *J Nucl Med.* 1977;18:1014–1021.
3. Segal AW, Arnot RN, Thakur ML, Lavender JP. Indium-111-labelled leucocytes for localisation of abscesses. *Lancet.* 1976;13:1056–1058.
4. Schauwecker DS, Burt RW, Park HM, et al. Comparison of purified indium-111 granulocytes and indium-111 mixed leukocytes for imaging of infections. *J Nucl Med.* 1988;29:23–25.
5. Datz FL, Thorne DA. Effect of chronicity of infection on the sensitivity of the In-111-labeled leukocyte scan. *AJR.* 1986;147:809–812.
6. Anstall HB, Coleman RE. Donor-leukocyte imaging in granulocytopenic patients with suspected abscesses: concise communication. *J Nucl Med.* 1982;23:319–321.
7. Dutcher JP, Schiffer CA, Johnston GS. Rapid migration of [111]indium-labeled granulocytes to sites of infection. *N Engl J Med.* 1981;304:586–589.
8. Schell-Frederick E, Fruhling J, Van der Auwera P, Van Laethem Y, Klastersky J. [111]Indium-oxine-labeled leukocytes in the diagnosis of localized infection in patients with neoplastic disease. *Cancer.* 1984;54:817–824.
9. O'Doherty MJ, Revell P, Page CJ, Lee S, Mountford PJ, Nunan TO. Donor leucocyte imaging in patients with AIDS: a preliminary report. *Eur J Nucl Med.* 1990;17:327–333.
10. Rojas-Burke J. Health officials reacting to infection mishaps. *J Nucl Med.* 1992;33:13N–14N, 27N.
11. Kaim A, Maurer T, Ochsner P, Jundt G, Kirsch E, Mueller-Brand J. Chronic complicated osteomyelitis of the appendicular skeleton: diagnosis with technetium-99m labelled monoclonal antigranulocyte antibody-immunoscintigraphy. *Eur J Nucl Med.* 1997;24:732–738.
12. Thakur ML, Lavender JP, Arnot RN, Silvester DJ, Segal AW. Indium-111-labeled autologous leukocytes in man. *J Nucl Med.* 1977;18:1014–1021.
13. Lillevang ST, Toft P, Nilsen B. A method for isolating granulocytes from rabbit blood without causing activation. *J Immunol Methods.* 1994;28:137–138.
14. Böyum A, Lövhaug D, Tresland L, Nordlie EM. Separation of leucocytes:

improved cell purity by fine adjustments of gradient medium density and osmolality. *Scand J Immunol.* 1991;34:697–712.

15. Joseph K, Damann V, Engeroff G, Gruner KR. Labeling of granulocytes with ^{99m}Tc-HMPAO: first clinical results [in German]. *Nucl Compact.* 1986;17:277–283.

16. Peters AM, Danpure HJ, Osman S, et al. Clinical experience with ^{99m}Tc-hexamethylpropylene-amineoxime for labelling leucocytes and imaging inflammation. *Lancet.* 1986;2:946–949.

17. Bach MC, Bagwell SP, Masur H. Utility of gallium imaging in the diagnosis of Mycobacterium avium-intracellulare infection in patients with the acquired immunodeficiency syndrome. *Clin Nucl Med.* 1986;11:175–177.

18. Bitran J, Bekerman C, Weinstein R, Bennett C, Ryo U, Pinsky S. Patterns of gallium-67 scintigraphy in patients with acquired immunodeficiency syndrome and the AIDS related complex. *J Nucl Med.* 1987;28:1103–1106.

19. Kramer EL, Sanger JJ. Detection of thoracic infections by nuclear medicine techniques in the acquired immunodeficiency syndrome. *Radiol Clin North Am.* 1989;27:1067–1076.

20. Kramer EL, Sanger JH, Garay SM, Grossman RJ, Tiu S, Banner H. Diagnostic implications of Ga-67 chest-scan patterns in human immunodeficiency virus-seropositive patients. *Radiology.* 1989;170:671–676.

21. Prvulovich EM, Miller RF, Costa DC. Immunoscintigraphy with a 99Tcm-labelled anti-granulocyte monoclonal antibody in patients with human immunodeficiency virus infection and AIDS. *Nucl Med Commun.* 1995;16:838–845.

22. Palestro CJ, Torres MA. Radionuclide imaging of nonosseous infection. *Q J Nucl Med.* 1999;43:46–60.

23. Ina K, Kusugami K, Yamaguchi T, et al. Mucosal interleukin-8 is involved in neutrophil migration and binding to extracellular matrix in inflammatory bowel disease. *Am J Gastroenterol.* 1997;92:1342–1346.

24. del Pozo MA, Sanchez-Mateos P, Nieto M, Sanchez-Madrid F. Chemokines regulate cellular polarization and adhesion receptor redistribution during lymphocyte interaction with endothelium and extracellular matrix: involvement of cAMP signaling pathway. *J Cell Biol.* 1995;131:495–508.

25. Springer TA. Traffic signals for lymphocyte recirculation and leukocyte emigration: the multistep paradigm. *Cell.* 1994;76:301–314.

26. Weiblen BJ, Forstrom L, McCullough J. Studies of the kinetics of indium-111-labeled granulocytes. *J Lab Clin Med.* 1979;94:246–255.

27. Deinard AS, Page AR. An improved method for performing neutrophil survival studies. *Blood.* 1970;36:98–110.

28. McMillan R, Scott JL. Leukocyte labeling with 51-chromium. I. Technic and results in normal subjects. *Blood.* 1968;32:738–754.

29. Dresch C, Najean Y, Bauchet J. Kinetic studies of ^{51}Cr and DF32P labelled granulocytes. *Br J Haematol.* 1975;29:67–80.

30. Athens JW. Granulocyte kinetics in health and disease. *Natl Cancer Inst Monogr.* 1969;30:135–155.

31. Dams ET, Nijhof MW, Boerman OC, et al. Scintigraphic evaluation of experimental chronic osteomyelitis. *J Nucl Med.* 2000;41:896–902.

32. Dams ET, Oyen WJ, Boerman OC, et al. Technetium-99m-labeled liposomes to image experimental colitis in rabbits: comparison with technetium-99m-HMPAO-granulocytes and technetium-99m-HYNIC-IgG. *J Nucl Med.* 1998;39:2172–2178.

33. Oyen WJ, Boerman OC, Dams ET, et al. Scintigraphic evaluation of experimental colitis in rabbits. *J Nucl Med.* 1997;38:1596–1600.